



International Symposium of Transport Simulation 2014

# On Microscopic Modelling of Adaptive Cruise Control Systems

Ioannis A. Ntousakis<sup>a</sup>, Ioannis K. Nikolos<sup>a\*</sup>, Markos Papageorgiou<sup>a</sup>

<sup>a</sup>*School of Production Engineering and Management, Technical University of Crete  
University Campus, GR-73100, Chania, Greece*

---

## Abstract

The Adaptive Cruise Control (ACC) system, is one of the emerging vehicle technologies that has already been deployed in the market. Although it was designed mainly to enhance driver comfort and passengers' safety, it also affects the dynamics of traffic flow. For this reason, a strong research interest in the field of modelling and simulation of ACC-equipped vehicles has been increasingly observed in the last years. In this work, previous modelling efforts reported in the literature are reviewed, and some critical aspects to be considered when designing or simulating such systems are discussed. Moreover, the integration of ACC-equipped vehicle simulation in the commercial traffic simulator Aimsun is described; this is subsequently used to run simulations for different penetration rates of ACC-equipped vehicles, different desired time-gap settings and different networks, to assess their impact on traffic flow characteristics.

© 2014 Published by Elsevier Ltd. Selection and peer-review under responsibility of ISTS 2014

*Keywords:* adaptive cruise control, ACC, traffic flow modelling, microscopic simulation.

---

## 1. Introduction

As we are advancing in the 21<sup>st</sup> century, new vehicle technologies arise, some of which affect not only safety and comfort of the passengers, but also traffic efficiency. The last decade has been a very productive one, since a continuing interdisciplinary effort has been made by the automobile industry and various governmental and research institutions around the world to plan, develop, and start deploying a variety of Vehicle Automation and Communication Systems (VACS) [Kesting et al., 2007; Shladover, 2012; Suzuki, 2003]. Although vehicle intelligence is increasing, one must not assume that traffic efficiency will automatically increase too; therefore modelling and simulation of such automation systems

---

\* Corresponding name: Ioannis K. Nikolos. Tel.: +30-28210-37300  
E-mail address: [jnikolo@dpem.tuc.gr](mailto:jnikolo@dpem.tuc.gr)

is needed, inter alia, for the systematic design and testing of future traffic control strategies. The first system that will potentially change significantly the dynamics of traffic flow is the adaptive cruise control (ACC) system [Kesting et al., 2007]. Various automotive companies have already introduced such systems, while several research teams have been working on their conceptual and numerical modeling [Darbha and Rajagopal, 1999; Rajamani et al., 2005; VanderWerf et al., 2001; Wang et al., 2013]. Regarding their microscopic modelling, issues to be considered are the control law of the ACC system, the number and meaning of its parameters, the impact of the response time and its string stability properties. Additional aspects, which are, however, outside the scope of this paper, could be safety implications, legal issues and technical restrictions, such as performance of ACC sensors in turning maneuvers, braking, hills, weather conditions etc. [Gurulingesh, 2004].

The first objective of this work is to summarize the available information in the existing literature for modelling and simulating of ACC-equipped vehicles. The second objective is to describe the development and evaluation of such a system, within the framework of one of the commercial microscopic traffic flow simulators. Aimsun, developed by Traffic Simulation Systems (TSS), was chosen for this work.

The review of available ACC systems and their simulation addresses the related control objectives, spacing selection policy, control laws and constraints. The different types of headway policy are examined, namely constant space-headway, constant time-headway, and variable time-headway. Moreover, the various control laws, proposed for controlling the longitudinal movement of ACC-vehicles, are briefly discussed, in order to conclude on the trends in the field.

Regarding the microscopic simulation framework used in this work, a short description of Aimsun is included, along with the corresponding API and MicroSDK tools. The details of the simulated networks and the respective car following models as well as the values of the parameters used for the conducted microscopic simulations are also described.

Finally, simulation results for two different cases are presented, to examine a) the impact of ACC on capacity for different penetration rates and different time-gap settings for an open-stretch road, and b) the effect of ACC on preventing the formation of stop-and-go waves in a ring-road. For the simulation of manually driven vehicles, two different models were applied, Gipps and IDM, the second one implemented using the MicroSDK platform of Aimsun.

## 2. Available models for ACC-equipped vehicles

### 2.1 Control approach and objectives

Regarding the control structure, a two-level (higher/ lower) approach is a common choice [Liang and Peng, 1999; Zhou and Peng, 2005]. The higher level deals with calculating the necessary or desired acceleration, depending on the vehicle's distance (range) to the leading vehicle and the difference in the corresponding velocities (range rate). The lower level deals with “transforming” the acceleration, computed at the higher level, into throttle or braking commands (figure 1). The control objectives should be the following [Shladover et al., 2012]:

- To travel with the maximum speed set by the driver in cases where there are no leading vehicles in the range covered by the sensors, or leading vehicles exist within that range but their velocities are higher than the maximum speed set by the user. This is also referred as *speed control mode* [Shladover et al., 2012].
- To maintain vehicle speed equal to the speed of the leading vehicle at a specified distance, when the leading vehicle is in range and its speed is lower than the maximum speed set by the driver. This is also referred to as *gap control mode* [Shladover et al., 2012].

- The transitions between the two aforementioned objectives should be as smooth as possible, in order not to cause discomfort to the passengers, e.g. due to abrupt accelerations or decelerations. Clearly, during lane-changing or cut-in maneuvers, a sudden change to the distance from the leading vehicle may occur, which may cause strong reactions from the system.

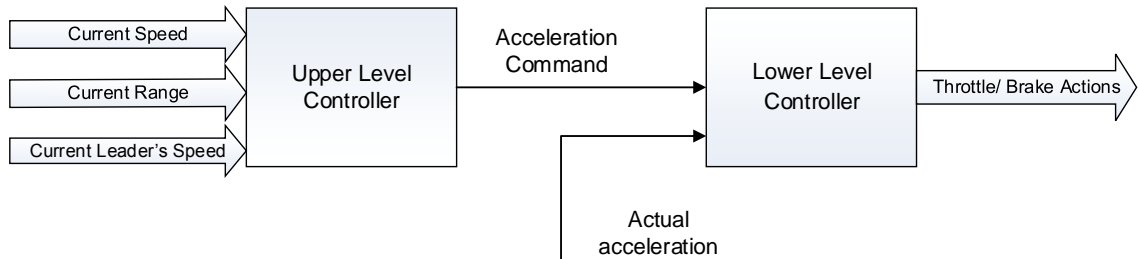


Fig. 1: Two-level ACC controller description.

In most of the existing modelling efforts, vehicles are considered “ideal”, meaning that the lower level controller does not exist, hence the acceleration command is applied instantaneously [Kesting et al., 2007; Shladover et al., 2012]. Even when the lower-level controller does exist, it is modelled as a simple first-order lag system, which appears sufficient for the purposes of controller design [Liang and Peng, 1999; VanderWerf et al., 2001]. When referring to stability of ACC systems, one should consider both the individual vehicle stability [Rajamani, 2012], as well as the string stability [Caudill and Garrard, 1977; Liang and Peng, 1999]. The first one ensures that the vehicle’s speed and acceleration do not oscillate, which would not only cause discomfort to the passengers but also possible problems or even permanent damage to the vehicle’s engine. The second one ensures that any perturbation in speed will not amplify as it propagates upstream, leading to unsafe gaps or oscillations [Liang and Peng, 1999; Swaroop and Hedrick, 1996]. Individual vehicle stability is obtained as long as the spacing error  $\delta_i$  (i.e. the difference between desired and actual gap from the preceding vehicle) after a possible perturbation converges to zero, given that the leading vehicle travels at a constant speed [Rajamani, 2012]. String (or platoon [Swaroop et al., 2001]) stability is obtained as long as all the spacing errors do not amplify as they travel upstream, which practically means that the energy of the spacing error  $\delta_i$  of vehicle  $i$  must be smaller compared to the energy of the error of its leading vehicle  $\delta_{i-1}$  [Rajamani, 2012]. Let  $\hat{H}(s)$  be the transfer function relating the spacing errors of consecutive vehicles  $i$  and  $i-1$ , defined by:

$$\hat{H}(s) = \frac{\delta_i}{\delta_{i-1}} \quad (1)$$

The corresponding impulse response function to  $\hat{H}(s)$  is defined as  $h(t)$ . String stability is achieved only if the transfer function satisfies the following constraints [Rajamani, 2012]:

$$\|\hat{H}(s)\|_{\infty} \leq 1 \quad (2)$$

$$h(t) > 0, \quad \forall t \geq 0. \quad (3)$$

## 2.2 Spacing selection policy

The spacing policy of ACC systems belongs to the most important factors, determining not only traffic flow characteristics but also vehicle safety [Lin et al., 2009]. Three main headway selection policies have been proposed: Constant Space-Headway (CSH), Constant Time-Headway (CTH) (space-headway is a linear function of speed) and Variable Time-Headway (VTH) (space-headway is a nonlinear function of speed) [Rajamani et al., 2005]. Although the first two policies are the simplest ones, the third is the subject of ongoing research and seems to offer plenty of room for further developments; the reader is referred to [Martinez and Canudas-de-Wit, 2007; Rajamani, 2012; Wang et al., 2013; Zhang and Ioannou, 2005; Zhou and Peng, 2005] for more information.

In order to avoid confusion, we need at this point to clarify the terms *headway* and *time-gap*; *time/space-headway* is the time/space distance between the front bumper of the preceding vehicle and the front bumper of the following vehicle, while *time/space-gap* is the time/space distance between the rear bumper of the preceding vehicle and the front bumper of the following one. These definitions are not always properly observed in the technical literature.

The CSH policy suggests that the inter-vehicle spacing should be constant for the whole speed range. However, it has been proven [Rajamani, 2012], [Darbha and Rajagopal, 1999] that this type of spacing policy is not string stable, unless additional information [Shladover, 1995] is received than the mere sensor data from the preceding vehicle. Therefore, it is not suitable for non-interconnected ACC systems and autonomous systems in general [Liang and Peng, 2000].

The CTH policy suggests that the inter-vehicle spacing should be a linear function of the vehicle's speed [Zhou and Peng, 2005]. Compared to the previously mentioned CSH policy, it feels more natural for the driver and the passengers, since the gap from the leading vehicle is proportional to its speed [Li and Shrivastava, 2002]. Although the results presented in [Darbha and Rajagopal, 1999] demonstrated that this policy can cause instabilities in an open stretch of highway with entries and exits, it has been shown through the use of a microscopic and two macroscopic approaches, applied both in a circular highway and in an open-stretch highway, that the string stability can be also guaranteed as long as a consistent downstream biasing strategy is applied [Li and Shrivastava, 2002]. This spacing policy can be simply described as follows:

$$L_{des} = s_0 + h_d v \quad (4)$$

where  $s_0$  is the jam distance in meters (gap between vehicles when completely stopped),  $h_d$  is the desired time-gap setting in seconds and  $v$  is the speed of the vehicle in m/s. Although in modelling and simulations the  $h_d$  setting can take any real value, the actual system installed in vehicles offers a choice between pre-defined desired time-gap settings, usually ranging between 0.8 s and 2.2 s [ISO 15622, 2010].

The third headway policy suggests that the inter-vehicle spacing should be a non-linear function of speed. The motivation to develop more complex spacing policies than the simple CTH one is to improve the dynamics and steady-state conditions of the system, in order to maximize the stability region, while increasing the capacity [Zhou and Peng, 2005]. Quite a few attempts to develop such policies have been reported so far. In [Zhou and Peng, 2005] the authors suggest a non-linear spacing policy, along with the related sliding mode controller; in their conducted simulations they realized that, in the presence of an on-ramp, CTH policy may become unstable, whereas their “quadratic range policy” ensures stability, despite the continuous disturbances from merging vehicles. The acceleration command is given by

$$a_{i,des} = \left(1 - \frac{\tau T_v}{T_a}\right) a_i + \frac{\tau}{T_a} \dot{R}_i + \frac{\tau \lambda}{T_a} \varepsilon_i \quad (5)$$

where  $\tau$  is the time constant of the servo-loop (vehicle dynamics),  $\dot{R}_i = v_{i-1} - v_i$  is the speed difference between the vehicle and its leader,  $T_v \equiv dR/dv$  is the equivalent time-headway,  $T_a$  is a positive parameter and  $\lambda$  is the convergence rate of the sliding surface, defined by  $\lambda = -\dot{S}/S$  where  $S = \varepsilon_i = R_i - (A + Tv_i + Gv_i^2) - T_a a_i$ ;  $A$  is the separation distance when vehicles have zero speeds (previously referred as  $s_0$ ),  $T$  and  $G$  are coefficients determined by curve fitting, which was applied on the data of a Field Operational Test [Fancher et al., 2003].

In [Rajamani et al., 2005] the authors outline the advantages of a non-linear spacing policy (Variable Time-Gap - VTG) compared to the CTH policy. They also verified that with the CTH policy traffic becomes unstable for significantly lower values of density, compared to the VTG, which practically means that with the VTG policy the range of densities for which traffic is stable is increased. In their results from simulations (the network was a pipeline plus an on ramp), they showed that a reduction of 44% in travel times can be achieved when a VTG strategy was employed. The acceleration command they propose is the following (vehicle dynamics were considered as a first-order lag, with a time constant  $\tau=0.1$  s)

$$\ddot{x}_{i,des} = -\rho_m(v_f - \dot{x}_i) \left(1 - \frac{\dot{x}_i}{v_f}\right) (\dot{\varepsilon}_i + \lambda \delta_i) \quad (6)$$

where  $\rho_m$  is a density parameter set as  $\rho_m=1/L$ , with  $L$  being the length of the vehicles, set to 5 m, and  $v_f$  is a velocity parameter set to 65 mph,  $\lambda$  is the convergence rate of the sliding surface, defined as:

$$\lambda = -\dot{\delta}_i/\delta_i. \quad (7)$$

Recently, in [Wang et al., 2013], a VTG policy was proposed in order to create a controller that takes vehicle safety explicitly into account, along with efficiency and comfort. By using the VTG policy, vehicles are supposed to keep larger gaps in lower densities and vice versa. The desired time-gap is given by

$$t_d = t_{d,0} + \frac{s}{s_f} (t_{d,m} - t_{d,0}) \quad (8)$$

where  $t_{d,0}$  is the minimum desired time-gap and  $t_{d,m}$  is the maximum desired time-gap (both set by the driver in order to include his preferences regarding the gap),  $s$  is the current gap and  $s_f$  is the gap threshold, which determines whether the vehicle is in cruising mode (speed control mode) or in following mode (gap control mode), and is given by:

$$s_f = v_0 t_{d,m} + s_0 \quad (9)$$

where  $v_0$  is the free speed, and  $s_0$  the inter-vehicle gap at standstill conditions (i.e. when the speeds are zero).

### 2.3 Limiting values and constraints of ACC systems

The correct modelling of an ACC system necessitates the limits and constraints of its various parameters and variables to be taken into account in a rational way. Firstly, the maximum acceleration and deceleration should be bounded, according to the vehicle's actual capabilities. Typical values for acceleration are 2-3 m/s<sup>2</sup> whereas for deceleration 3-5 m/s<sup>2</sup>. In [ISO 15622, 2010] it is recommended that for ACC systems the average automatic acceleration should not exceed 2 m/s<sup>2</sup> whereas the deceleration should not exceed 3.5 m/s<sup>2</sup>. The previous values should possibly be additionally bounded by constraints, in order to prevent the driver from feeling uncomfortable (i.e. too strong accelerations or decelerations).

Regarding speed, it should be bounded by the minimum of the following values: maximum speed of the vehicle, maximum acceptable speed by the driver, and maximum allowed speed of the highway section (possibly multiplied by a “speed acceptance” coefficient in order to model various types of drivers). The range of vehicle sensors is another critical parameter of ACC systems; typical values for state of the art sensors’ range are between 150 m and 200 m [Kesting, 2008; Wang et al., 2013] while typical sampling rates are in the range of 77 GHz [Kesting, 2008].

Safety is a critical factor that should be taken into account in the design process of such a system. According to [Wang et al., 2013] the most critical situation an ACC-vehicle can encounter is to approach a stopped vehicle at free flow speed. This means that the range of the sensors must be sufficient in order to be able to come to a safe full stop by applying the maximum deceleration, once the obstacle is detected. This constraint however is not included in most of the design efforts [Wang et al., 2013]. The transition mechanism between speed and gap control modes is also quite significant regarding comfort. This means that during the transition phase the acceleration or deceleration should remain as smooth as possible. In most of the design efforts in the literature, the transition mechanism is absent or not reported; there are however some studies that include a transition mechanism [Kesting et al., 2010; Rajamani, 2012; Shladover et al., 2012].

#### 2.4 ACC Control Laws

The existing control laws, used to control the velocities of ACC-equipped vehicles by implementing the CTH policy will be discussed in brief; although differences exist between them, they share common basic ideas. The control objective is to eliminate the range error (error between actual and desired inter-vehicle distance) and the velocity error (difference between the speeds of leader and follower).

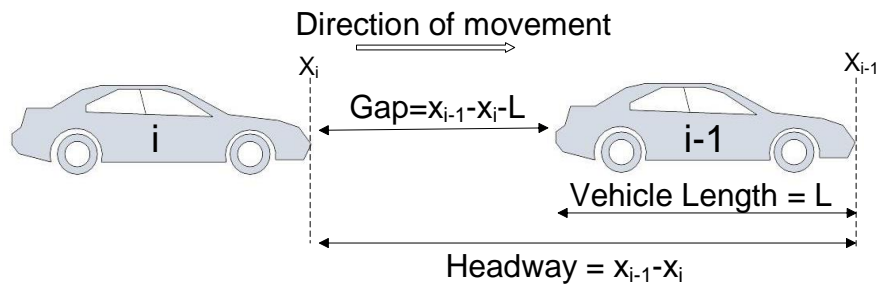


Fig. 2: Schematic representation of the basic car following parameters.

In [Liang and Peng, 1999] the authors suggest the following control law for ideal vehicles:

$$\ddot{x}_i = K_1(x_{i-1} - x_i - h_d v_i) + K_2(v_{i-1} - v_i) \quad (10)$$

$$\ddot{x}_{i-1} = K_1(x_{i-2} - x_{i-1} - h_d v_{i-1}) + K_2(v_{i-2} - v_{i-1}) \quad (11)$$

where index  $i-1$  refers to the leader of vehicle  $i$ ,  $x_i$  is the position of vehicle  $i$ ,  $\ddot{x}_i$  is the acceleration of vehicle  $i$ ,  $v_i$  is its speed,  $h_d$  is the desired time-headway in seconds and  $K_1, K_2$  are the control gains. In this case, since vehicles are ideal, the acceleration command  $u_i$  is equal to  $\ddot{x}_i$ , which means that it is followed instantaneously and vehicle dynamics are not taken into account. The control gains should be calculated in a way that on one hand guarantees string stability and on the other hand maximizes performance (in terms of minimizing the range and range rate errors). The proposed optimal values for the gains are

$K_1=1.12$  and  $K_2=1.70$ . For non-ideal vehicles, the authors modelled the dynamics of the vehicle as a first order lag system, where:

$$\dot{a}_k = \frac{1}{\tau_\alpha} (u_k - a_k). \quad (12)$$

It was proven that, if the above mentioned control law (equations 10, 11) was applied for ideal vehicles, the results were similar to the case where the following control law (equation 13) was applied for non-ideal vehicles:

$$\ddot{x}_k = \frac{1}{\tau_\alpha} [K_1(x_{k-1} - x_k - h_d \dot{x}_k) + K_2(\dot{x}_{k-1} - \dot{x}_k) - \ddot{x}_k]. \quad (13)$$

In this case the computed optimal gains were  $K_1=0.83$  and  $K_2=1.26$ . String stability was proven to be also guaranteed in the case of non-ideal vehicles.

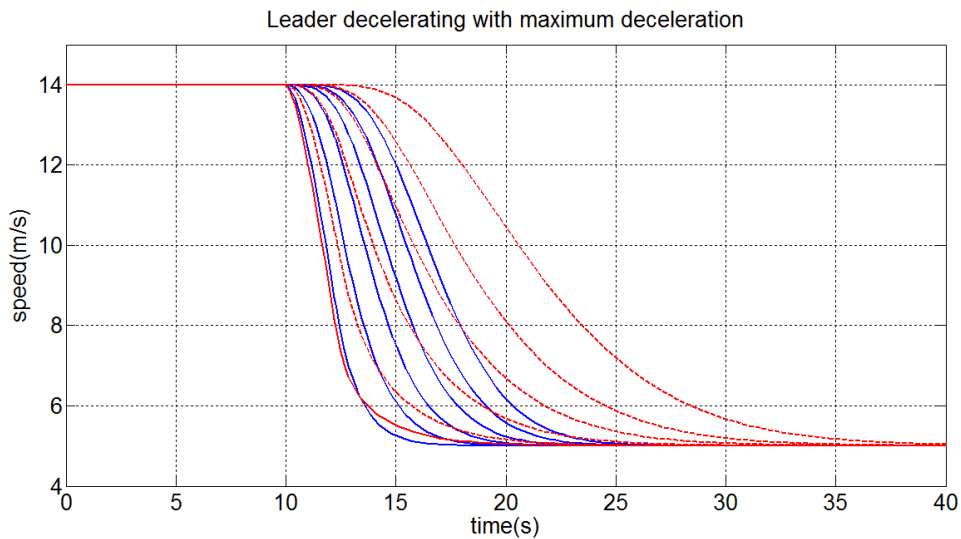


Fig. 3: Speed response of six following vehicles when the leader decelerates with the maximum deceleration for two different parameter settings. The solid line (blue) is the response for  $K_1 = 1$  and  $K_2 = 0.2$  and the dashed (red) for  $K_1 = 1.12$ ,  $K_2 = 1.7$ . (For both cases  $\alpha=3 \text{ m/s}^2$ ,  $b=4 \text{ m/s}^2$ , and time-headway equal to 1 s.)

In figure 3, the response of six following vehicles when the leader decelerates (with a constant deceleration of  $4 \text{ m/s}^2$ ) from  $14 \text{ m/s}$  to  $5 \text{ m/s}$  is presented for the case of equation (10). The example was plotted with two different parameter combinations in order to visualize the impact they have on vehicle dynamics.

Since ACC system's response time is in the order of  $0.1$  to  $0.2 \text{ s}$  [Kesting et al., 2007], compared to substantially larger human driver reaction times, suitable ACC models produce acceleration commands that are a continuous function of the velocity, range, and range rate. Also, according to [Kesting et al., 2007], a model intended to simulate ACC-equipped vehicles should meet the following criteria:

- It must be accident-free.
- The car-following dynamics should represent a smooth driving style, which would feel natural and safe for the passengers.

- The transitions when vehicles cut-in, or change lane or in any way modify the traffic situation must be non-oscillatory.
- Few parameters should be needed, permitting easy calibration.
- It should be able to model different driving styles (e.g. aggressive or relaxed etc.) and it should take into account the vehicle's constraints in terms of maximum acceleration, deceleration, speed etc.

Based on the above, it is suggested in [Kesting et al., 2007] that the Intelligent Driver Model (IDM) [Treiber et al., 2000] is suitable for modelling and simulating ACC-equipped vehicles. The equations forming the model are the following

$$\dot{v}(s, v, \Delta v) = a \left[ 1 - \left( \frac{v}{v_0} \right)^4 - \left( \frac{s^*(v, \Delta v)}{s} \right)^2 \right] \quad (14)$$

$$s^*(v, \Delta v) = s_0 + vT + \frac{v\Delta v}{2\sqrt{ab}} \quad (15)$$

where  $a$  is the maximum acceleration,  $b$  is the desired deceleration,  $v_0$  is the free flow speed,  $s_0$  is the jam distance (distance between vehicles when stopped),  $T$  is the safe time-gap. The IDM model has been implemented as an ACC system in a Volkswagen test car [Kesting, 2008].

IDM model - Leader decelerating with maximum deceleration

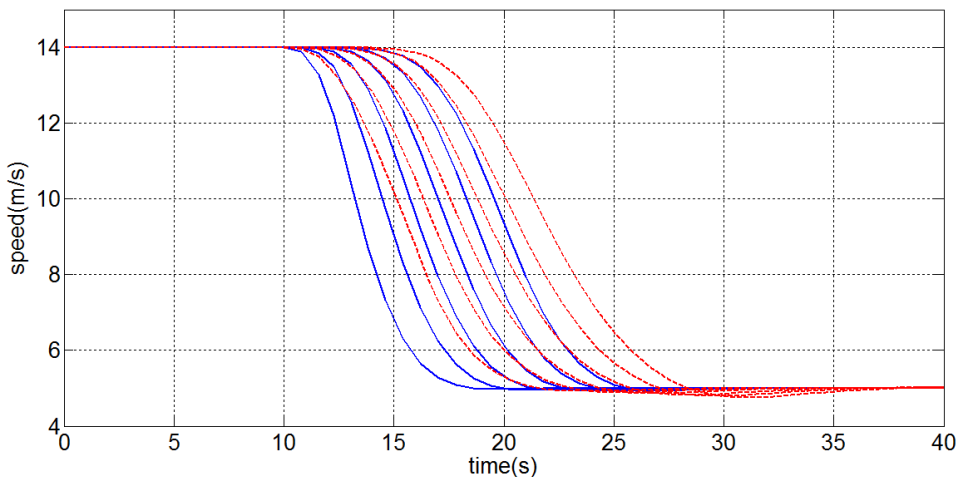


Fig. 4: Speed response of six following vehicles when the leader decelerates with constant deceleration for two different parameter settings. The solid line (blue) is the response for  $\alpha = 3 \text{ m/s}^2$  and  $b = 4 \text{ m/s}^2$  and the dashed (red) for  $\alpha = 1 \text{ m/s}^2$  and  $b = 1.5 \text{ m/s}^2$  (time-headway equal to 1 s).

In figure 4, the response of the IDM model for an example where the leader decelerates with maximum deceleration from 14 m/s to 5 m/s is presented. The example was executed with two different parameter combinations (maximum acceleration deceleration) in order to visualize the impact they have on vehicle dynamics.

The model of [Shladover et al., 2012] is a simplified version of the ACC control laws that were actually applied on test cars and are proprietary to Nissan. The authors separate the control law in two

parts: speed control and gap control. Speed control is applied when the distance from the leading vehicle is larger than 120 m, while gap control uses the CTH policy and is applied when the distance from the preceding vehicle is smaller than 100 m. When the distance is between 100 m and 120 m, the vehicle retains the previous control law (hysteresis), in order to avoid chattering between the two control laws. The corresponding equations are listed below

*Speed control:*

$$\begin{aligned} v_e &= v - v_d \\ a_{sc} &= \text{bound}(-0.4 \cdot v_e, 2, -2) \\ a &= a_{sc} \end{aligned} \quad (16)$$

*Gap control:*

$$\begin{aligned} v_e &= v - v_d \\ a_{sc} &= \text{bound}(-0.4 \cdot v_e, 2, -2) \\ s_d &= T_d \cdot v \\ s_e &= s - s_d \\ \alpha &= \text{bound}(\dot{s} + 0.25 \cdot s_e, a_{sc}, -2) \end{aligned} \quad (17)$$

and

$$\text{bound}(x, x_{ub}, x_{lb}) = \max(\min(x, x_{ub}), x_{lb}) \quad (18)$$

where  $v$  is the speed of the ACC-vehicle,  $v_d$  is the desired speed set by the driver or speed limit of the section,  $v_e$  is the speed error,  $a_{sc}$  is the acceleration in speed control mode,  $s$  is the spacing between the ACC-vehicle and its leader,  $s_d$  is the desired spacing,  $s_e$  is the spacing error and  $T_d$  is the desired time-gap. The values +2 and -2 are the maximum acceleration and deceleration under ACC control, respectively.

Comparing the gap control law with the previous one [Liang and Peng, 1999], one can observe that it can take the form:

$$a = \dot{s} + 0.25(s - T_d \cdot v) \xrightarrow[\substack{\dot{s}=v_{i-1}-v_i \\ s=x_{i-1}-x_i}]{\substack{\dot{s}=v_{i-1}-v_i \\ s=x_{i-1}-x_i}} \ddot{x}_i = 0.25(x_{i-1} - x_i - T_d \cdot v) + (v_{i-1} - v_i) \quad (19)$$

which is equivalent to the one used in [Liang and Peng, 1999] with  $K_1=0.25$  and  $K_2=1$ . The time constant used for “achieving” the desired speed is 2.5 s, which, according to the authors, leads to a typical gentle ACC response. The model they used for simulating manual vehicles is the car-following part of the complete NGSIM oversaturated freeway flow model [Yeo et al., 2008], since there were no lane-changings in the simulations.

According to [Davis, 2004a], the dynamics of an ACC-vehicle, can be modelled through the following set of equations. The index  $n-1$  refers to the leader of the vehicle  $n$ .

$$\tau \frac{dv_n(t)}{dt} + v_n(t) = V(\Delta x_n(t), \Delta v_n(t)) \quad (20)$$

$$\Delta x_n(t) = x_{n-1}(t) - x_n(t) \quad (21)$$

$$\Delta v(t) = v_{n-1}(t) - v_n(t). \quad (22)$$

Vehicle response is modelled as a first-order system, with a time constant  $\tau$  with values around 0.5 to 1.0 seconds. Using the constant time-headway policy, the desired inter-vehicle distance is given by

$$\Delta x_n^{desired}(t) = h_d v_n(t) + D \quad (23)$$

where  $h_d$  is the desired time-gap in seconds and  $D$  is a constant length equal to the vehicle length plus the space between the vehicles when they are completely stopped. The function  $V$  is defined as:

$$V = \frac{1}{h_d} [\Delta x_n(t) - D] + \beta \Delta v_n(t). \quad (24)$$

The parameter  $\beta$  (coefficient of the rate of change) is chosen as  $\beta = \tau/h_d$ .

$$\varepsilon_n(t) = v_n(t) - V_d(\Delta x_n(t)) \quad (25)$$

$$V_d(\Delta x) = \frac{1}{h_d} (\Delta x - D). \quad (26)$$

Based on the findings of [Liang and Peng, 1999], Davis proved [Davis, 2004a] that his control law is also string stable. For the simulations, he did not use bounds for acceleration or deceleration but only for speed  $0 < V < V_{max} = (35 \text{ m/s})$ ; he executed simulations with and without on-ramps for single- and multilane freeways. The model used for manual vehicles was the modified optimal velocity model [Davis, 2004b].

In [Ioannou and Chien, 1993], the vehicle model used is described by the following equations

$$\frac{d}{dt} x_i(t) = \dot{x}_i(t) = v_i(t) \quad (27)$$

$$\frac{d}{dt} \dot{x}_i(t) = \ddot{x}_i(t) = a_i(t) \quad (28)$$

$$\frac{d}{dt} \ddot{x}_i(t) = b(\dot{x}_i, \ddot{x}_i) + a(\dot{x}_i) u_i(t) \quad (29)$$

where:

$$a(\dot{x}_i) = \frac{1}{m_i \tau_i(\dot{x}_i)} \quad (30)$$

$$b(\dot{x}_i, \ddot{x}_i) = -2 \frac{k_{d_i}}{m_i} \dot{x}_i \ddot{x}_i - \frac{1}{\tau_i(\dot{x}_i)} \left[ \ddot{x}_i + \frac{k_{d_i}}{m_i} \dot{x}_i^2 + \frac{d_{m_i}(\dot{x}_i)}{m_i} \right] \quad (31)$$

$x_i$  is the position of the  $i_{th}$  vehicle in meters,  $v_i$  is the velocity of the  $i_{th}$  vehicle in m/s,  $a_i$  is the acceleration of the  $i_{th}$  vehicle in  $\text{m/s}^2$ ,  $m_i$  is the mass of the  $i_{th}$  vehicle in kg,  $\tau_i$  is the  $i_{th}$  vehicle's time-constant in seconds,  $u_i$  is the  $i_{th}$  vehicle's engine input,  $k_{d_i}$  is the  $i_{th}$  vehicle's aerodynamic drag coefficient in kg/m, and  $d_{m_i}$  is the  $i_{th}$  vehicle's mechanical drag coefficient. The used control law is described as

$$u_i(t) = \frac{1}{a(\dot{x}_i)} [c_i(t) - b(\dot{x}_i, \ddot{x}_i)] \quad (32)$$

where

$$c_i(t) = C_p \delta_i(t) + C_u \dot{\delta}_i(t) + K_v v_i(t) + K_\alpha \alpha_i(t) \quad (33)$$

$$\delta_i(t) = x_{i-1}(t) - x_i(t) - (L_i + S_{o_i} + \lambda_2 v_i(t)) \quad (34)$$

$$\dot{\delta}_i(t) = v_{i-1} - v_i - \lambda_2 \alpha_i(t). \quad (35)$$

$L_i$  is the length of vehicle  $i$ ,  $S_{d_i}(t)$  is the desired safety spacing in meters,  $S_{0_i}$  is the spacing at time  $t=t_0$  equal to  $S_{d_i}(t_0)$ ,  $\delta_i(t)$  is the spacing error (deviation from the desired safe spacing), and  $\lambda_2$  is a constant representing the constant time-headway in seconds;  $C_p$ ,  $C_u$ ,  $K_v$ ,  $K_a$  are design constants which are chosen taking into account the following considerations: a) stability, b) steady-state performance, c) slinky-type effects avoidance, and d) oscillatory behaviour avoidance.

For simulations, a constant (i.e not a function of the vehicle's operation point) engine time-constant is used, equal to 0.25 s for half of the vehicles and 0.3 s for the other half. They also used different sampling times for the radar sensors, ranging from 0.1 s to 0.3 s and did not notice any significant difference regarding the acceleration response. In this work, the maximum acceleration, deceleration and jerk constraints were ignored.

In [VanderWerf et al., 2001] the authors also adopt a controller identical to that of [Liang and Peng, 1999] with the addition of limiting acceleration and deceleration to acceptable values.

### 3. The simulation environment

#### 3.1 The microscopic simulator

The implementation of ACC models in commercial traffic simulators is possible when the simulators include modules which offer users the ability to override the default car-following models and apply alternative ones. For the purposes of this (and subsequent) work(s), the microscopic simulator Aimsun [Transport Simulation Systems, 2013a] was used to develop the ACC model and perform the corresponding simulations. Aimsun also includes the Aimsun API [Transport Simulation Systems, 2013b], and MicroSDK [Transport Simulation Systems, 2013c] tools, which can be used to extend its capabilities.

The Aimsun API module offers the possibility to extend the functionalities of the basic Aimsun simulation environment by including user-defined applications in C++ or Python. The user has access to almost all necessary information during simulation, such as measurements of detectors or the speeds and positions of particular vehicles etc. Therefore the developed applications can have direct communication and interaction with the simulator and exchange the necessary data. Additionally, the Aimsun microscopic simulator includes the MicroSDK tool, which, among others, allows for the modification or replacement of the incorporated car-following models. For each simulation step, Aimsun calls the appropriate functions and updates the vehicle data based on the user-defined behavioural model. For the purposes of this work, we mainly used the MicroSDK tool, in order to apply the new models, and the API to retrieve the results as data files.

#### 3.2 Car-Following models

The default car-following model implemented in Aimsun is based on the Gipps model [Gipps, 1981; Gipps, 1986]. It can be actually considered as a slightly modified version of this empirical model, in which the model parameters are not global but determined both by the vehicle's and driver's characteristics (maximum desired acceleration and deceleration, speed limit acceptance etc.), by influence of local parameters (speed limit on the section, speed limits on turnings, etc.), the influence of vehicles on adjacent lanes, etc. It consists of two speed components, one for acceleration and one for deceleration. The first represents the intention of a vehicle to achieve a certain desired speed, while the second reproduces the limitations imposed by the preceding vehicle when trying to drive at the desired speed.

The model states that the maximum speed to which a vehicle ( $i$ ) can accelerate during a time period ( $t, t+T$ ) is given by

$$V_a(i, t + T) = V(i, t) + 2.5a(i)T \left(1 - \frac{V(i, t)}{V^*(i)}\right) \sqrt{0.025 + \frac{V(i, t)}{V^*(i)}} \quad (36)$$

where  $V(i, t)$  is the speed of the vehicle  $i$  at time  $t$ ,  $V^*(i)$  is the desired speed of vehicle  $i$  for the current section,  $a(i)$  is the maximum desired acceleration of vehicle  $i$ , and  $T$  is the reaction time of the vehicle. On the other hand, the maximum speed that the same vehicle ( $i$ ) can reach during the same time interval ( $t, t+T$ ), according to its own characteristics and the limitations imposed by the presence of the lead vehicle (vehicle  $i-1$ ) is

$$V_b(i, t + T) = d(i)T + \sqrt{d^2(i)T^2 - d(i) \left[ 2\{x(i-1, t) - s(i-1) - x(i, t)\} - V(i, t)T - \frac{V(i-1, t)^2}{d'(i-1)} \right]} \quad (37)$$

where  $d(i)$  is the maximum deceleration desired by vehicle  $i$  (negative value),  $x(i, t)$  is the position of vehicle  $i$  at time  $t$ ,  $s(i-1)$  is the effective length of vehicle  $i-1$ , that is the physical length plus a margin into which the following vehicle is not willing to intrude, even when at rest;  $d'(i-1)$  is an estimation of the desired deceleration of  $i-1$  vehicle. For each simulation step, vehicles are updated with the minimum of the previously mentioned speeds  $V_a, V_b$ .

The control law used in this work for the ACC-vehicles [Rajamani et al., 2005] is described below

$$\begin{aligned} \ddot{x}_{i,des} &= -\frac{1}{h_d}(\dot{\varepsilon}_i + \lambda\delta_i) \\ \varepsilon_i &= x_i - x_{i-1} \\ \delta_i &= x_i - x_{i-1} + L_i + h_d\dot{x}_i \\ d(i) &\leq \ddot{x}_{i,des} \leq a(i) \\ 0 &\leq \dot{x}_i \leq V^*(i) \end{aligned} \quad (38)$$

and can take the following form, similar to the one used in [Liang and Peng, 1999],

$$\ddot{x}_{i,des} = \frac{1}{h_d}(\dot{x}_{i-1} - \dot{x}_i) + \frac{\lambda}{h_d}(x_{i-1} - x_i - L_i - h_d\dot{x}_i) \quad (39)$$

with  $K_1 = \lambda/h_d$   $K_2 = 1/h_d$ . The reasons for applying this control law for ACC-equipped vehicles is its simplicity and its adoption (in slightly different forms) by various researchers.

## 4. Simulation examples

### 4.1 Example 1: Open stretch

The network used for simulations is a single-lane 4km stretch without any on-ramps or off-ramps. The speed limit at the section is 120 km/h, the simulated time was 15 minutes, and the output data and measurements were stored after the first 3 minutes (warm-up period). ACC-equipped vehicles have the same mean values for maximum acceleration and deceleration as the manually-driven cars. Since Aimsun assigns these values randomly for each vehicle, vehicles are not identical, but their parameter values follow the same distribution. The reaction time for manual vehicles is 0.7 s whereas for ACC-vehicles is 0.1s; the simulation step is set to 0.1 s.

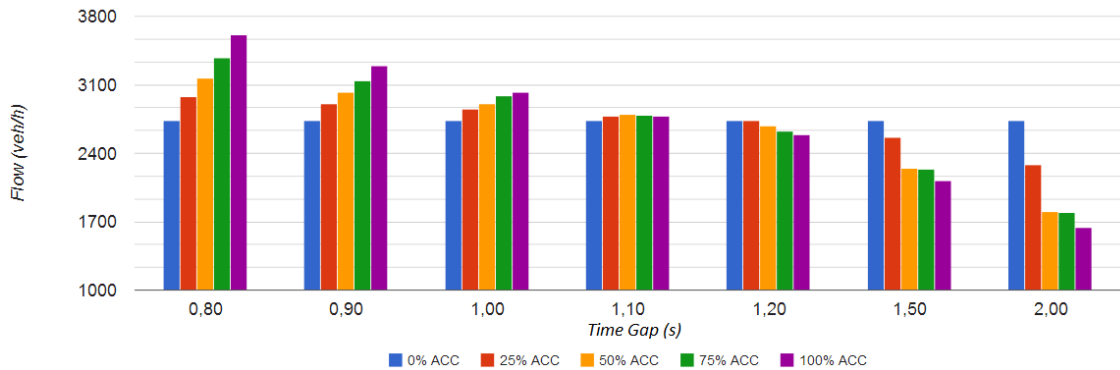


Fig. 5: Flow for different desired time-gap settings and different penetration rates of ACC-vehicles (open-stretch case).

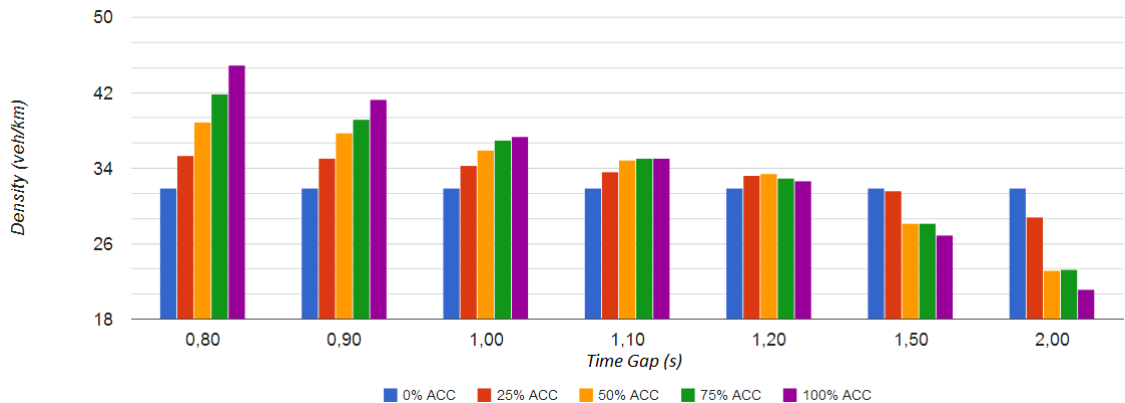


Fig. 6: Density for different desired time-gap settings and different penetration rates of ACC-vehicles (open-stretch case).

Experiments were conducted for different desired time-gap settings and different penetration rates. The penetration rate took the values 0%, 25%, 50%, 75%, 100%, the parameter  $\lambda$  was set to 0.2, as in [Rajamani et al., 2005], and the time-headway took the values 0.8 s, 0.9 s, 1.0 s, 1.1 s, 1.2 s, 1.5 s, and 2.0 s. This resulted in a total of 29 different simulation scenarios. Each scenario was executed 10 times (replications) in order to take also into account the stochastic nature of the simulations. The demand was sufficiently large (so that some vehicles were left out in a virtual queue), and, as a result, the measured flow equals capacity (figure 5). The average density is illustrated in figure 6. The number of vehicles that managed to enter the network (i.e. Total demand – left out vehicles) are illustrated in figure 7.

In figure 5 it can be noticed that the capacity increases with ACC penetration rate as long as the time-gap setting is less than 1.10 s - 1.20 s. In cases where this value is higher, the capacity decreases with the penetration rate. It is obvious from figure 5, that a high ACC penetration rate combined with a long desired time-gap setting could lead to a very low capacity. This is one example of why traffic management is vital in presence of new technologies in vehicles.

In figure 6 it is observed that density increases with the penetration rate as long as the time-gap setting is less than 1.10 s. This is expected and it is due to the fact that inter-vehicle spacing is smaller compared to manual vehicles. Figure 7 is a direct result of the graphs in figures 5 and 6, since it proves that more vehicles managed to enter the network when the time-gap setting is small and the penetration rate is high, which of course is due to the improved capacity.

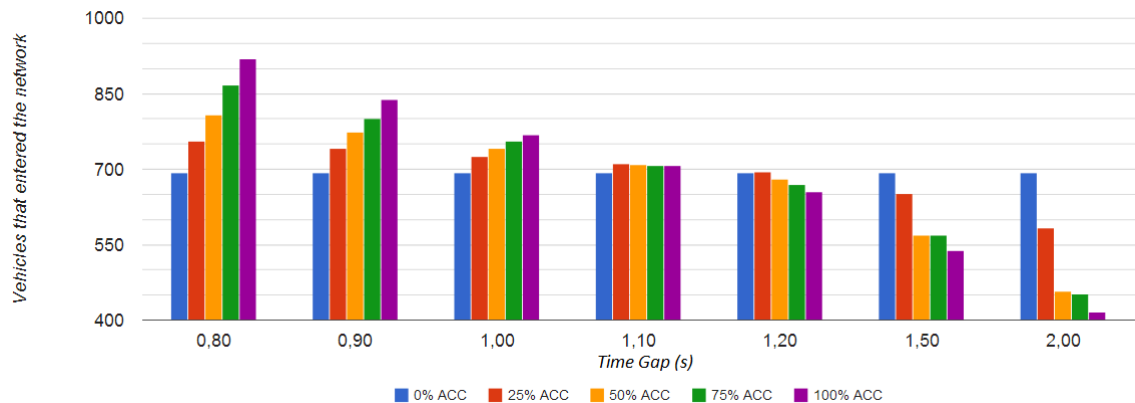


Fig. 7: Number of vehicles that managed to enter the network for different desired time-gap settings and different penetration rates of ACC-vehicles (open-stretch case).

#### 4.2 Example 2: Ring-road

The second example refers to a ring-road; a single-lane, 4 km ring-road was used to test the stability of the ACC system compared to manually-driving. Testing was done using both the default Aimsun model (Gipps) as well as the IDM model, for manual vehicles. The reason the IDM model was adopted for manual vehicles is that it can replicate stop-and-go waves [Treiber and Kesting, 2013], contrary to the Gipps model [Barcelo, 2010], which was not able to replicate such waves in our experiments (results for the Gipps model are not included for brevity reasons).

For ACC-vehicles, the same control law was used as in the previous simulation example. The network was initially loaded with 200 identical vehicles, leading to a mean density of 50 veh/km. Detectors were placed every 50 m and aggregated density measurements were collected every 20 s. Once the traffic became almost uniform, a perturbation was applied, through the deceleration of a vehicle for 60 s and its subsequent acceleration. The result was a wave propagating upstream (figure 8). Two different sub-cases were considered; for the first one, a maximum acceleration for the IDM model equal to  $a=1.35$  m/s<sup>2</sup> was used (figures 8, 9), while for the second one, a maximum acceleration  $a=1.8$  m/s<sup>2</sup> was used (figures 10, 11). The same maximum acceleration was used for both manual and ACC-equipped vehicles in the conducted experiments. The remaining parameters of the IDM model were:  $s_0 = 2$  m,  $v_0 = 33.33$  m/s and the time-headway was set to  $T=1.5$  s. The space-time diagrams of density are illustrated for 100% manual vehicles modelled with the IDM model (figures 8 and 10) and for 50% manual vehicles modelled

with the IDM model and 50% ACC-vehicles (figures 9 and 11), modelled with the control law described in section 3.2.

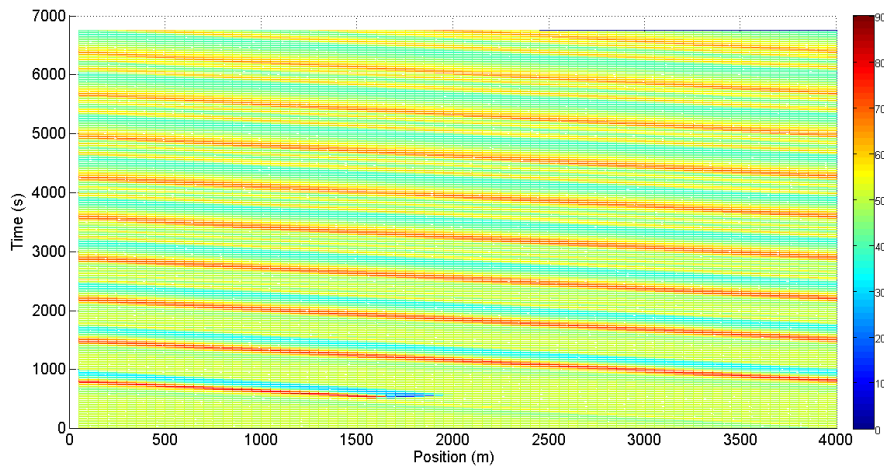


Fig. 8: Density evolution with time for the ring-road example, using the IDM model with  $\alpha = 1.35 \text{ m/s}^2$  (100% manually-driven vehicles).

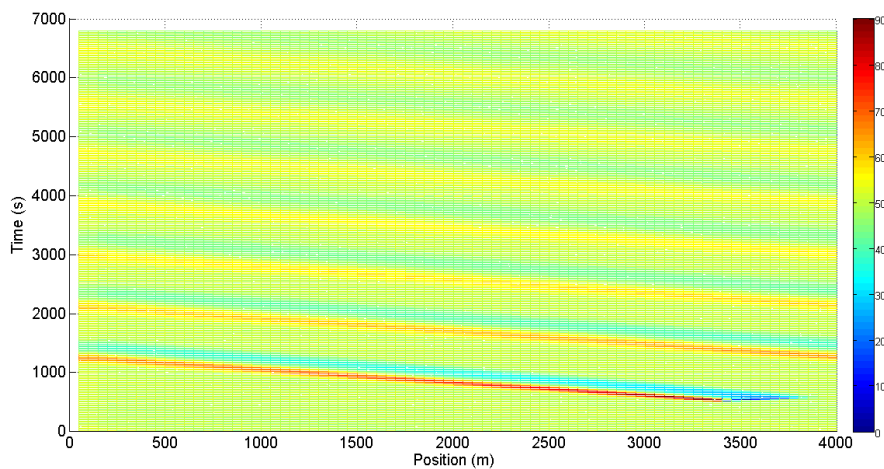


Fig. 9: Density evolution with time for the ring-road example (50% manually-driven vehicles modelled with the IDM model with  $\alpha = 1.35 \text{ m/s}^2$ , and 50% ACC-equipped vehicles).

In figure 8, the initial speed perturbation produces a density perturbation at time  $\sim 700 \text{ s}$ , which propagates upstream and eventually is producing multiple stop-and-go waves. The presence of ACC-equipped vehicles (at a penetration rate of 50%) significantly reduced this phenomenon, as it is depicted in figure 9. The density perturbation fades-out quickly, and no multiple stop-and-go waves are formed. The phenomenon is less pronounced for the second sub-case ( $\alpha=1.8 \text{ m/s}^2$ , figures 10, 11). However, the

presence of ACC-equipped vehicles has an observable smoothing effect on the oscillations, in this case also.

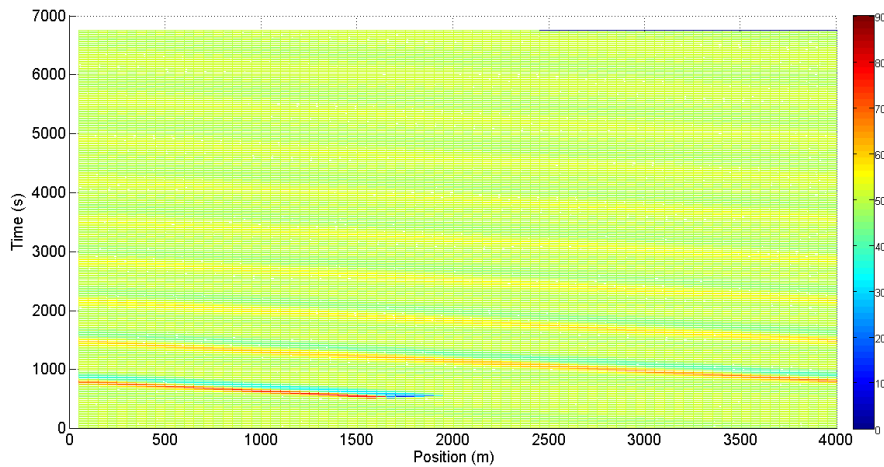


Fig. 10: Density evolution with time for the ring-road example, using the IDM model with  $\alpha = 1.8 \text{ m/s}^2$  (100% manually-driven vehicles).

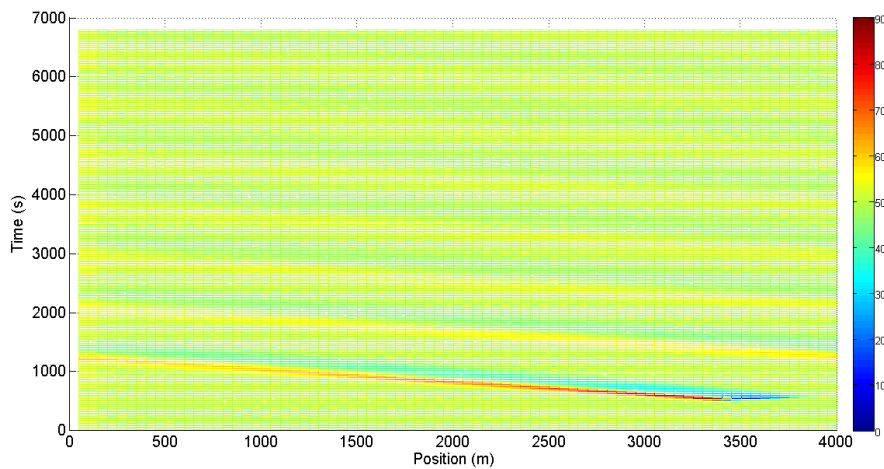


Fig. 11: Density evolution with time for the ring-road example (50% manually-driven vehicles modelled with the IDM model with  $\alpha = 1.8 \text{ m/s}^2$ , and 50% ACC-equipped vehicles).

## 5. Conclusions

This work consists of two main parts; the first one contains an extended literature survey regarding the modelling efforts of various research groups for ACC systems, focusing not only on the control laws but also on the spacing policy. The second part describes the modelling of ACC-equipped vehicles in the

commercial traffic simulator Aimsun and its use for investigating the impact of ACC-vehicles on traffic flow. A short description of the simulator and its additional tools is also provided. Simulations were executed for different penetration rates of ACC-vehicles, as well as for different desired time-gap settings. The results showed that the desired time-gap setting has direct impact on the capacity: The smaller the time-gap setting, the higher the capacity. Additionally, a large ACC penetration rate can improve the capacity as long as the desired time-gap setting is smaller than that of manual vehicles. If this is not the case, then one can observe deterioration in terms of capacity. This highlights the need for the correct use of ACC systems, with regard to traffic management. A second example was executed, in a ring-road in order to verify the stabilizing effects of ACC systems, when the boundary conditions are periodic. It was observed that ACC-vehicles can improve the stability of traffic, since they mitigate the intensity and number of stop-and-go waves.

Through this work, two possible areas with a high research interest were identified. The first one, is the spacing policies and in particular the VTG policies. Although there is some literature on the topic, there is plenty of room for further research. The second one, is to investigate in depth the interaction between manual and ACC-equipped vehicles, also in a multi-lane environment. Although the behaviour of an automated system can be estimated and modelled quite accurately, the behaviour of the drivers of manual vehicles in presence of automated ones is still an open issue.

## Acknowledgements

This research was supported by TRAMAN21 (TRAFFIC MANAgement for the 21st Century) ERC Advanced Investigator Grant under the European Union's Seventh Framework Programme.

## References

- Caudill, R.J., Garrard, W.L., 1977. Vehicle-Follower Longitudinal Control for Automated Transit Vehicles. *J. Dyn. Syst. Meas. Control* 99, 241.
- Darba, S., Rajagopal, K., 1999. Intelligent cruise control systems and traffic flow stability. *Transp. Res. Part C Emerg. Technol.* 7, 329–352.
- Davis, L., 2004a. Effect of adaptive cruise control systems on traffic flow. *Phys. Rev. E* 69, 066110.
- Davis, L., 2004b. Multilane simulations of traffic phases. *Phys. Rev. E* 69, 016108.
- Fancher, P., Bareket, Z., Peng, H., Ervin, R., 2003. Research on desirable adaptive cruise control behavior in traffic streams. Phase 2 Final Report. UMTRI-2013-14.
- Gipps, P.G., 1981. A behavioural car-following model for computer simulation. *Transp. Res. Part B Methodol.* 15, 105–111.
- Gipps, P.G., 1986. A model for the structure of lane-changing decisions. *Transp. Res. Part B Methodol.* 20, 403–414.
- Gurulingesh, R., 2004. Adaptive Cruise Control. M.Sc. Thesis. Kanwal Rekhi School of Information Technology, Indian Institute of Technology Bombay.
- Barcelo, J., 2010. Models, Traffic Models, Simulation, and Traffic Simulation. In Hillier, F.S. (Ed.), *Fundamentals of Traffic Simulation*, International Series in Operations Research & Management Science. Springer New York.

- Ioannou, P.A., Chien, C.C., 1993. Autonomous intelligent cruise control. *IEEE Trans. Veh. Technol.* 42, 657–672.
- ISO 15622, 2010. Intelligent transport systems - Adaptive Cruise Control systems - Performance requirements and test procedures.
- Kesting, A., 2008. Microscopic Modeling of Human and Automated Driving: Towards Traffic-Adaptive Cruise Control. Doctoral Thesis. Technical University of Dresden. Germany.
- Kesting, A., Treiber, M., Helbing, D., 2010. Enhanced intelligent driver model to access the impact of driving strategies on traffic capacity. *Philos. Trans. A. Math. Phys. Eng. Sci.* 368, 4585–605.
- Kesting, A., Treiber, M., Schönhof, M., Helbing, D., 2007. Extending Adaptive Cruise Control to Adaptive Driving Strategies. *Transp. Res. Rec.* 2000, 16–24.
- Li, P.Y., Shrivastava, A., 2002. Traffic flow stability induced by constant time headway policy for adaptive cruise control vehicles. *Transp. Res. Part C Emerg. Technol.* 10, 275–301.
- Liang, C.-Y., Peng, H., 1999. Optimal Adaptive Cruise Control with Guaranteed String Stability. *Veh. Syst. Dyn.* 32, 313–330.
- Liang, C.-Y., Peng, H., 2000. String Stability Analysis of Adaptive Cruise Controlled Vehicles. *JSME Int. J. Ser. C* 43, 671–677.
- Lin, T.-W., Hwang, S.-L., Green, P. a., 2009. Effects of time-gap settings of adaptive cruise control (ACC) on driving performance and subjective acceptance in a bus driving simulator. *Saf. Sci.* 47, 620–625.
- Martinez, J.-J., Canudas-de-Wit, C., 2007. A Safe Longitudinal Control for Adaptive Cruise Control and Stop-and-Go Scenarios. *IEEE Trans. Control Syst. Technol.* 15, 246–258.
- Rajamani, R., 2012. *Vehicle Dynamics and Control*, Mechanical Engineering Series. Springer US, Boston, MA.
- Rajamani, R., Levinson, D., Michalopoulos, P., Wang, J., Santhanakrishnan, Kumaragovindhan Zou, X., 2005. Adaptive Cruise Control System Design And Its Impact on Traffic Flow. University of Minnesota, Department of Civil Engineering. Project Report CTS 05-01.
- Shladover, S.E., 1995. Review of the State of Development of Advanced Vehicle Control Systems (AVCS). *Veh. Syst. Dyn.* 24, 551–595.
- Shladover, S.E., 2012. Recent International Activity in Cooperative Vehicle – Highway Automation Systems. The Exploratory Advanced Research Program, U.S. Department of Transportation, FHWA-HRT-12-033.
- Shladover, S.E., Su, D., Lu, X.-Y., 2012. Impacts of Cooperative Adaptive Cruise Control on Freeway Traffic Flow. *Transp. Res. Rec. J. Transp. Res. Board* 2324, 63–70.
- Suzuki, H., 2003. Effect of adaptive cruise control (ACC) on traffic throughput: numerical example on actual freeway corridor. *JSAE Rev.* 24, 403–410.
- Swaroop, D., Hedrick, J.K., 1996. String stability of interconnected systems. *IEEE Trans. Automat. Contr.* 41, 349–357.
- Swaroop, D., Hedrick, J.K., Choi, S.B., 2001. Direct adaptive longitudinal control of vehicle platoons. *IEEE Trans. Veh. Technol.* 50, 150–161.
- Treiber, M., Hennecke, A., Helbing, D., 2000. Congested traffic states in empirical observations and microscopic simulations. *Phys. Rev. E* 62, 1805–1824.

- Treiber, M., Kesting, A., 2013. *Traffic Flow Dynamics*. Springer Berlin Heidelberg, Berlin, Heidelberg.
- Transport Simulation Systems (TSS), 2013a *Aimsun 8 Dynamic Simulators Manual*.
- Transport Simulation Systems (TSS), 2013b *Aimsun 8 API Manual*.
- Transport Simulation Systems (TSS), 2013c *Aimsun 8 MicroSDK Manual*.
- VanderWerf, J., Shladover, S., Kourjanskaia, N., Miller, M., Krishnan, H., 2001. Modeling Effects of Driver Control Assistance Systems on Traffic. *Transp. Res. Rec.* 1748, 167–174.
- Wang, M., Daamen, W., Hoogendoorn, S.P., van Arem, B., 2013. Rolling horizon control framework for driver assistance systems. Part I: Mathematical formulation and non-cooperative systems. *Transp. Res. Part C Emerg. Technol.*
- Yeo, H., Skabardonis, A., Halkias, J., Colyar, J., Alexiadis, V., 2008. Oversaturated Freeway Flow Algorithm for Use in Next Generation Simulation. *Transp. Res. Rec. J. Transp. Res. Board* 2088, 68–79.
- Zhang, J., Ioannou, P., 2005. Adaptive Vehicle Following Control System with Variable Time Headways, in: *Proceedings of the 44th IEEE Conference on Decision and Control*. IEEE, pp. 3880–3885.
- Zhou, J., Peng, H., 2005. Range Policy of Adaptive Cruise Control Vehicles for Improved Flow Stability and String Stability. *IEEE Trans. Intell. Transp. Syst.* 6, 229–237.